Underwater superoleophobic biomaterial based on waste potato peels for simultaneous separation of oil/water mixtures and dye adsorption

Arun K. Singh ⬥ · Shruti Mishra · Jayant K. Singh

Abstract Underwater superoleophilicity involves interactions between a solid surface and two immiscible liquids, viz., water and oils, in which water remains in the completely wetted and oils in the non-wetted state. Materials with underwater superoleophilicity have drawn significant interest due to their superior performance in selective separation of oil and organic solvents from an aqueous phase. However, the development of such materials with special wettability for water and oils are hindered by (1) complex fabrication process (2) long processing duration with high cost, and (3) use of environmentally unfriendly and expensive fluorochemicals to lower the surface energy. Herein, we demonstrate the use of waste potato peels (WPP) to fabricate simple, economical and eco-friendly materials with superhydrophilic (water contact angle $\sim 0°$) and underwater superoleophobic (oil contact angle $> 150°$) properties.

Initially, powder of WPP was prepared and accumulated into a layer via a simple cleaning, smashing, one step inexpensive chemical treatment and stacking procedures. The developed WPP layer was efficient for the gravity-driven separation of various oil/water mixtures (including hexane, toluene, dodecylbenzene, and kerosene) and water-in-oil emulsions, with high efficiency ($> 98\%$) in single unit operation. During the oil/water separation process, the WPP layer was also found to serve as an adsorbent material for efficient removal of various water-soluble dyes (methylene blue and rhodamine B, 50 mg L^{-1}) contaminants, simultaneously. Thus, the developed WPP layer is not only a good biomaterial for water remediation by the oil/water separation and dye adsorption simultaneously, but can also contribute in reducing environmental pollution and wastage.
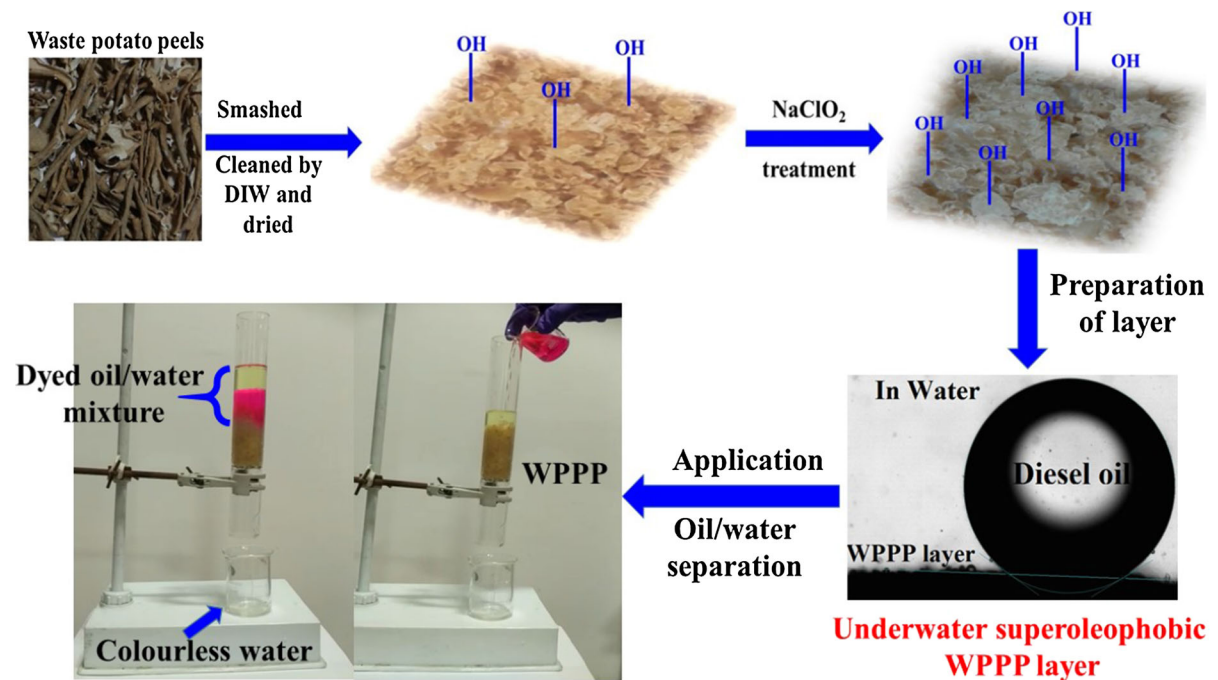
A. K. Singh · S. Mishra · J. K. Singh (✉)
Department of Chemical Engineering, Indian Institute of Technology Kanpur, Kanpur 208016, India
e-mail: jayantks@iitk.ac.in

Graphical abstract

Introduction

Nature provides numerous examples to bring creativity in engineering design for solving man-made problems (Si et al. 2018). One such class of example is the design of superhydrophobic (water-repellent) surfaces. There are various examples of natural biomaterial viz., lotus leaf, butterfly wings and water strider leg, which possess special features (superhydrophobic properties) that are sources of inspiration for engineering design of innovative substrates for various applications (Das et al. 2018; Gao and Jiang 2004; Ueda and Levkin 2013; Marmur 2012; Zhou et al. 2016). Inspired by naturally water-repellent surfaces in the recent years, there has been substantial effort to mimic those surfaces with artificial superhydrophobicity, owing to their promising potential for various applications, such as in anti-icing, anti-

corrosion, anti-fogging, self-cleaning and also in oil/water separation (Singh and Muller-Plathe 2014; Nguyen et al. 2018; Song et al. 2018; Sukamanchi et al. 2017; Schlaich et al. 2016).

In recent years, with the rapid expansion of variety of industries, frequent oil spillages and leakage of oil and organic solvents, a large amount of oily wastewater has been released into the environment, which is a significant environmental hazard as well as wastage of water resources (Baig et al. 2018; Wang and Wang 2018; Qu et al. 2018). Moreover, oily wastewater from dye production chemical plants such as dyeing industry, textile printing, and pulp industry usually contains a lot of water-soluble toxic dyes, which can cause severe environmental pollution and tremendous human health risk (Baig et al. 2018; Qu et al. 2018; Cao et al. 2016; Wen et al. 2019). Thus, it is of great significance to develop an effective approach which can be useful to separate water-insoluble oily contaminants as well as water-soluble toxic dyes simultaneously from the wastewater coming from various sources before discharging.

It is well known that the separation of oil/water mixtures is governed by the interfacial phenomenon, and thus materials with superhydrophobic-superoleophilic or

superhydrophilic-superoleophobic properties are of great interest to separate oil–water mixture (Li et al. 2016; Singh and Singh 2019). The superhydrophobic-superoleophilic surfaces have the ability to prevent the passage of water, whereas it allows the oil to pass through easily (Singh and Singh 2016, 2017a). Thus, in the recent past, several research studies have been conducted to develop superhydrophobic surfaces for oil–water mixture separation applications. For instance, superhydrophobic and superoleophilic nanostructured layer on the steel mesh (Khosravi and Azizian 2017), zirconia-siloxane coated superhydrophobic cotton fabric (Singh and Singh 2017b), furfuryl alcohol modified hydrophobic melamine sponge (Feng et al. 2017), and superhydrophobic GO/AgBr coated copper mesh (Zhu et al. 2017) have been reported for the separation of oil/water mixtures. While the aforementioned superhydrophobic-superoleophilic surfaces offer a better solution for the separation of oil/water mixtures, pores of these materials are easily blocked (fouling) by the oils, during oil/water separation, because of its superoleophilicity. The blocked pores are hard to clean consequently reduces the efficiency and reusability of the superhydrophobic materials for oil/water separation (Wang and Wang 2018; Qu et al. 2018).

In order to overcome the issues discussed above, various workers developed materials with superhydrophilicity and underwater superoleophobicity for oil–water separation, inspired by natural biologically underwater oil-repellent surfaces such as short clam shells, fish scales, and seabirds (Qu et al. 2018; Liu et al. 2012, 2009). Such specific materials have the ability to prevents the passage of oils, and allows water to pass through easily, thus, completely avoids oil fouling. For example, Zhu et al. 2018, fabricated underwater superoleophobic stainless steel fiber felts via nanoparticles deposition [$Cu(OH)_2$ nanoneedles] and electrochemical oxidation methods, and the prepared mesh exhibited high separation efficiency (> 99%) of oil/water mixtures. You et al. 2018, prepared Zn–ZnO electrodeposited copper mesh with superhydrophilic and underwater superoleophobic via electrodeposition process, which also could separate oil/water mixtures with 99% separation efficiency in corrosive, alkali and acidic environments. Although these developed superhydrophilic/underwater superoleophobic surfaces are highly efficient for oil/water separation, the fabrication process is expensive, sophisticated, and require special equipment.

Moreover, such materials are mainly effective in separating insoluble oily contaminants from water, and cannot remove water-soluble organic contaminants (dyes) simultaneously. It should be noted that the oily wastewater discharged from dyeing and textile industry usually contains significant water-soluble toxic dyes, which must be removed before discharging in order to avoid environmental pollution. Therefore, it is of great significance to develop special materials with superhydrophilicity and underwater superoleophobicity via facile, inexpensive and scalable approach for efficient separation of water-insoluble oil/organic solvents and water-soluble dyes contaminants simultaneously.

The potato peel is one of the typical green biomass cellulose based materials, consisting of biodegradable, nontoxic and massive amphiphilic substances such as starch (25%), nonstarch polysaccharide (30%), acid insoluble and acid soluble lignin (20%), protein (18%), lipids, long chain fatty acids (1%), and ash (6%) (Linag and McDonald 2014; Camire et al. 1997; Guechi and Hamdaoui 2016). Due to extensive use of potato in various applications such as starch production, and in food processing industries, huge quantity of potato peels is being generated as a waste, which has negligible economic value, and thus poses a disposal problem leading to serious environmental pollution for water, soil, and air (Zhang et al. 2015). Because of its special amphiphilic components, it would be more valuable if the potato peels are used to prepare desired material (superhydrophilic and underwater superoleophobic) for oil/water separation and removal of water-soluble dyes. Recently, cellulose nanocrystal based membranes with superhydrophilic and underwater superoleophobic properties have been reported for highly efficient oil/water separation with good recyclability (Zhan et al. 2018a, b; Cheng et al. 2017).

With this in mind, in this work, waste potato peel powder (WPPP) with superhydrophilicity and underwater superoleophobicity was developed into a layer via simple cleaning, smashing of waste potato peels, one step $NaClO_2$ treatment and stacking procedures. It was noted that the prepared WPPP layer acted as "water removing" type filtrate material with an excellent special wettability (underwater superoleophobicity). Thus, the developed WPPP layer was used in the gravity-driven separation of various immiscible oil/water mixtures (including hexane, toluene,

dodecylbenzene, and kerosene) and water-soluble dyes contaminants (methylene blue and rhodamine B). In addition, the WPPP layer has been also verified to effectively separate water-in-oil emulsions. Furthermore, the generated WPPP layer shows an excellent separation capacity ($>98\%$) for selected immiscible oil/water mixtures, water-in-oil emulsions and can adsorb methylene blue and rhodamine B water-soluble dyes, simultaneously. Thus, the development of WPPP layer from a waste via a simple inexpensive process, and without any use of toxic chemicals is a feasible strategy for water remediation applications.

Experimental section

Materials

Waste potato peels were obtained from mess halls of IIT Kanpur. Sodium chlorite ($NaClO_2$) was used as a modifying agent which was purchased from Sigma Aldrich. Oxalic acid, ethanol, dodecylbenzene, n-hexane, and toluene (analytical grade) were supplied by Rankem. Diesel and kerosene were purchased from a local store (Kanpur, India). Water soluble dyes such as methylene blue and Rhodamine B were also purchased from Rankem. A variety of solutions such as water-in-oil emulsion and dye solutions were prepared using distilled water. Other solvents and chemicals were used as received without further purification.

Preparation of waste potato peels powder (WPPP) and its treatment process

Waste potato peels (WPP) were initially cleaned ultrasonically with distilled water in a repeated manner to remove the impurities. After this, cleaned WPP were dried in an electric oven to reduce the moisture content. Finally, the WPP were crushed into tiny granule powder and sieved to get the size of particles in the range of 0.5 μm–2.0 mm. The obtained WPPP in the above process was further treated with sodium chlorite ($NaClO_2$) (Wang and Wang 2018).

In this treatment process, initially 200 mL homogenous aqueous solution of $NaClO_2$ (2 wt%) was prepared, and the pH of this solution was adjusted to 4.5 by adding oxalic acid. Subsequently, we immersed WPPP (10 g) in the solution, and the solution was

placed under a magnetic stirring which was kept at 80 °C. After the reaction for 2 h, the product was filtered and washed with distilled water several times. The obtained $NaClO_2$-treated WPPP was dried and stored for further characterization and applications.

Preparation of waste potato peels layer

Figure 1 illustrates the preparation process of WPPP and its layer for application in oil/water separation with adsorption of water-soluble dyes. In this process, the $NaClO_2$-treated WPPP was stacked in the form of a layer in a sintered glass filter tube as shown in Fig. 1. The diameter of this layer was 3 cm, and two pieces of nylon mesh (300 mesh size) of appropriate size were used to support this layer (similar to a sandwich) on both ends (lower and upper) to prevent the loss of materials during the filtration process.

Water purification

Evaluation of immiscible oil/water mixtures and emulsion separation efficiency

In order to evaluate the oil/water separation capability, the as-prepared $NaClO_2$ treated WPPP was fixed into the sintered glass tube in the form of a layer as shown in Fig. 1. Initially, the layer of WPPP was wetted with water. After that, oil/water mixtures (1:1, V/V) were poured slowly into the glass tube, and this mixture was passed through the layer by the force of gravity. Five types of organic solvents and oils including diesel, kerosene, hexane, dodecylbenzene, and toluene were used to prepare oil–water mixtures.

In addition, two different types of surfactant-free water-in-oil emulsions were prepared by the use of toluene and dodecylbenzene. These two water-in-oil emulsions were prepared by the sonication of 1 mL of water and 100 mL toluene (or dodecylbenzene) and vigorously stirring of water/oil mixtures. Similar to the immiscible oil/water mixture, these emulsions were poured onto the WPPP layer to achieve the separation.

Application in dye removal

In order to evaluate the water-soluble dyes removal property of WPPP layer, homogeneous aqueous solutions of methylene blue and rhodamine B dyes (50 mg L^{-1}) were prepared by dissolving the desired
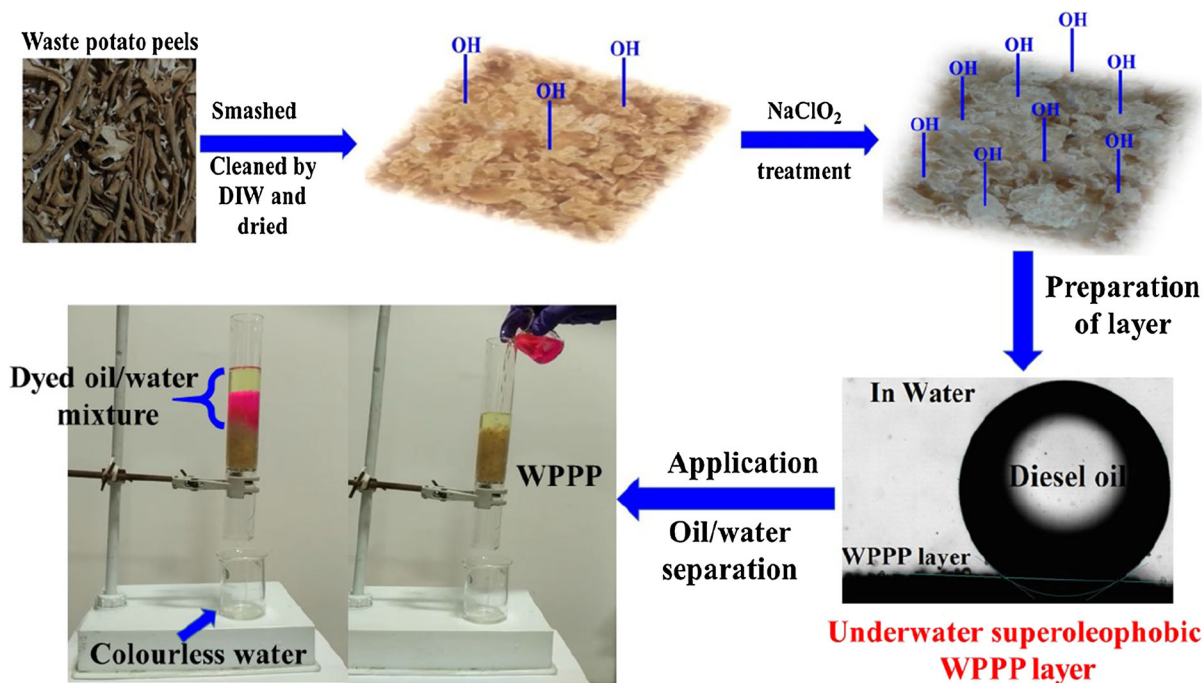
Fig. 1 Illustration of the preparation process of WPPP layer and its application for the simultaneous separation of oil–water mixtures and adsorption of water-soluble dyes

amount of dyes with 1000 mL water in a volumetric flask. Hereafter, the dye solutions were used to prepare oil–water (1:1, v/v) mixtures with diesel oil. Subsequently, as-prepared oil/water mixtures with 50 mg L^{-1} concentration of dyes were used for investigating the water-soluble dyes removal property of the WPPP layer via the filtering experiment. The UV–Visible spectrophotometer was used to measure the dye concentration difference between the dye solution and their respective filtrate after one step permeation through the WPPP layer.

Characterizations

The surface morphology of the as-prepared WPPP was analyzed by field emission scanning electron microscopy (FESEM, Zeiss, Germany, supra-40VP). Before the analysis of surface morphology, a sputtering coater was used to place the thin layer of gold film on the samples in order to prevent charging (Singh et al. 2017). Fourier transformed infrared (FTIR) spectra were recorded using FTIR spectrometer (KBR pellet method) in the range of 500–4000 cm^{-1} in order to identify the presence of functional groups on the surface of original and treated WPPP. The

superhydrophilicity and underwater superoleophobicity (wetting behavior) of WPPP were examined by the measurement of water contact angle (WCA) and underwater oil contact angle (OCA) using goniometer (OCA 20, DataPhysics, Germany) instrument by sessile liquid drop method at the room temperature. The values of WCA and OCA were measured in five different spots on the same sample surface and the mean value of the contact angles was used. The distribution of water droplets in the water-in-oil emulsion was evaluated by the images of optical microscopy (Carl Zeiss). The concentration of water-soluble dyes before and after filtration through WPPP layer was measured with Agilent Cary 60 UV–Visible spectrophotometer.

Results and discussion

Surface morphology and chemical composition of the as-prepared WPPP layer

In this study, WPPP was used to separate immiscible oil/water mixtures, water-in-oil emulsions and water-soluble dyes with oil/water separation simultaneously.
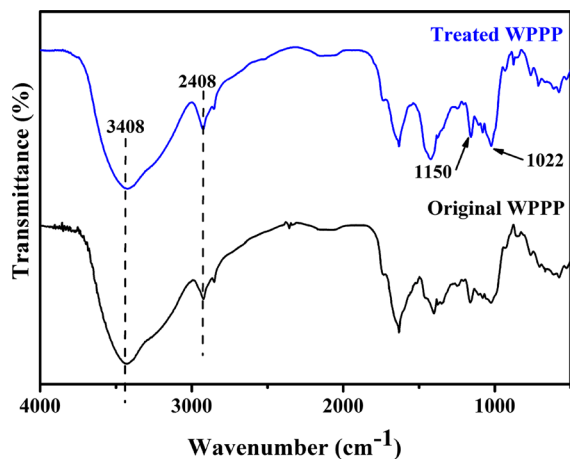
Initially, the waste potato peels (WPP) were cleaned with distilled water, as shown in Fig. 2a. After cleaning, WPP was dried at room temperature and smashed into powder (Fig. 2b). Subsequently, the WPP powder (WPPP) was treated with $NaClO_2$ solution, to prepare $NaClO_2$-treated WPPP. Moreover, the surface morphologies of $NaClO_2$-treated WPPP were examined by the FE-SEM measurements. The FE-SEM images of WPPP in different magnification (low and high) are shown in Fig. 2c, d. The surface of WPPP exhibits a typical rough structure instead of a smooth surface. The WPPP showed rough surface because of its random arrangement in layer-by-layer

packaged structure in which surface of particles is covered with many grooves and apertures.

Figure 3 displays the FTIR spectra of original and $NaClO_2$-treated WPPP over the range of 4000–500 cm^{-1}. The peaks at 1150 and 1022 cm^{-1} are assigned to the C–O and –CH_2 related modes (Arampatzidou and Deliyanni 2016). In the spectra of both original and treated WPPP, the broad peak at 3408 cm^{-1} is related to the stretching vibration of hydroxyl groups (Wang and Wang 2018). However, from the spectra, it was observed that the intensity of this peak at 3408 cm^{-1} increases significantly in the case of $NaClO_2$-treated WPPP, as compared to original (untreated) WPPP. This observation confirms
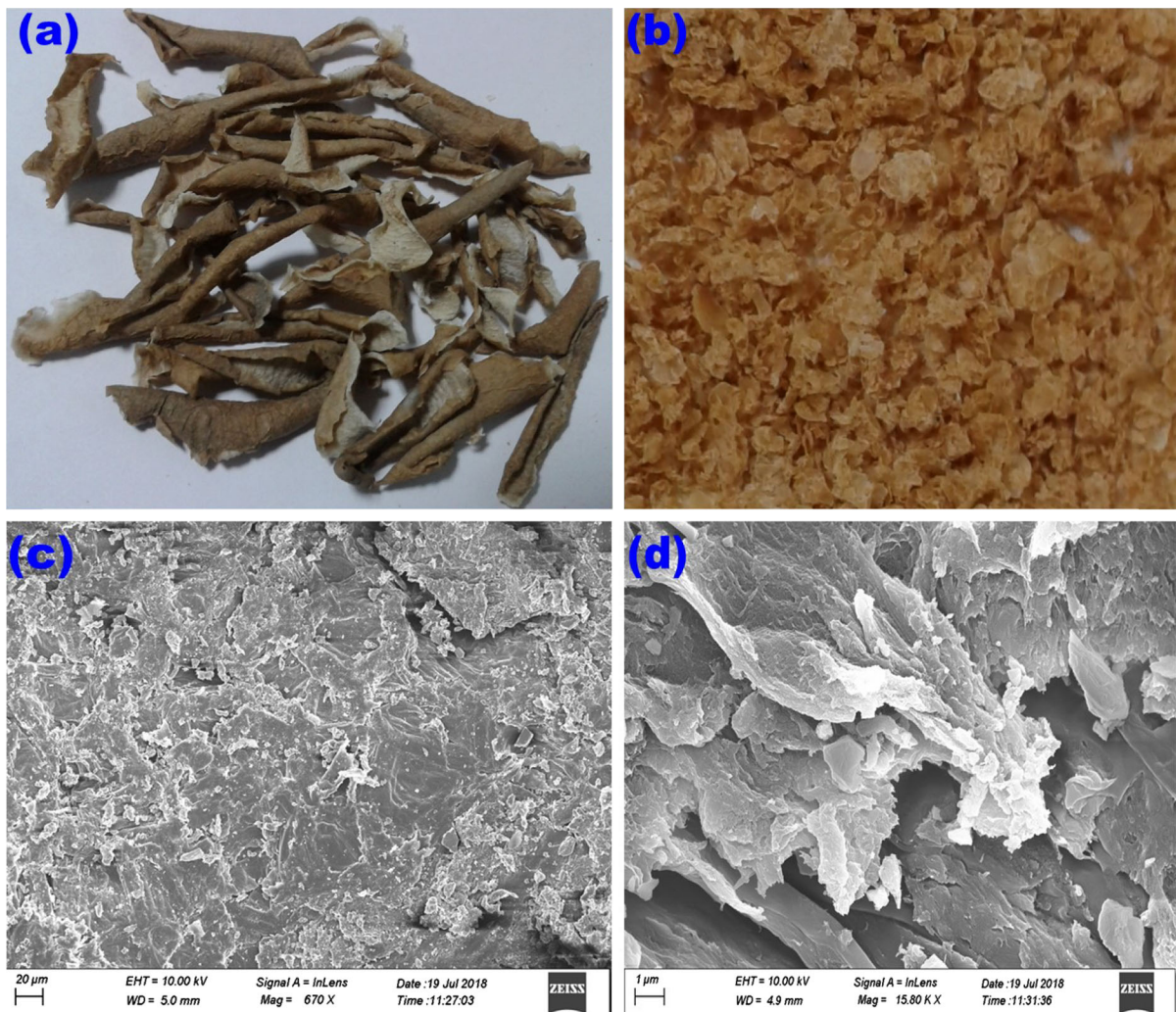
Fig. 2 a Photographs of waste potato peel. b The potato peel after being smashed, cleaned, $NaClO_2$ treated and dried. c, d The FE-SEM images of waste potato peel powder (WPPP) with different magnification
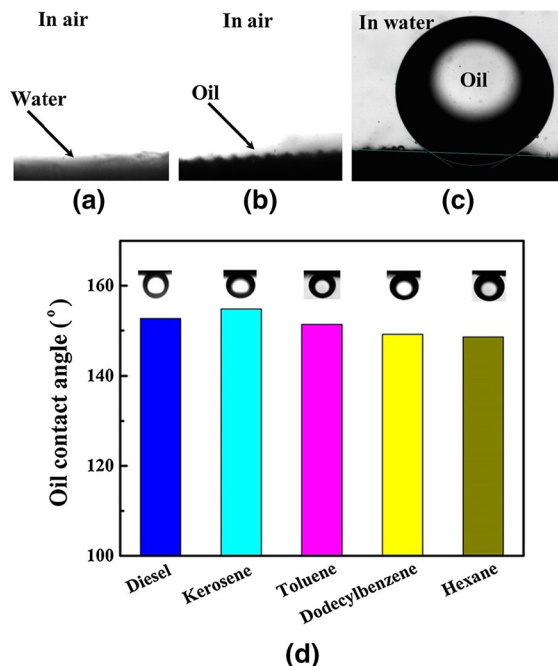
Fig. 3 The FTIR spectra of original and NaClO$_2$-treated WPPP

Fig. 4 Wetting behaviours of the WPPP layer towards **a** water in air, **b** oil in air and **c** oil in underwater, **d** oil contact angle (OCA) for various underwater oil droplets on the surface of NaClO$_2$-treated WPPP layer

that more hydroxyl groups exposed on the surface of WPP after the simple treatment with NaClO$_2$. This exposure of hydroxyl groups leads to improvements in hydrophilicity of the WPPP (Arampatzidou and Deliyanni 2016).

Wettability performance of the as-prepared WPPP layer

The wetting behaviour of NaClO$_2$ treated WPPP was evaluated in the air by the measurement of contact angles with water and oils at the room temperature by the sessile liquid drop method using goniometer (OCA 20, DataPhysics, Germany) instrument. Initially, a thick and dense layer of WPPP was prepared by spreading it on the glass slide. When water and oil droplets were dripped onto the treated WPPP surface, the droplets were immediately absorbed, and the surface gets wet within few seconds, as exhibited in Fig. 4a, b. Thus, the treated WPPP exhibits superhydrophilic and superoleophilic (superamphiphilicity) property in the air with both water and oil contact angles (CA) of nearly 0° (Fig. 4a, b).

The wetting behaviour of any solid surface governed by the geometrical structure and its chemical composition (Li et al. 2016). In the case of WPPP, high affinity with water and oil is because of its constituents such as starch and cellulose. Thus, when the amphiphilic WPPP surface is immersed in the water, the water permeates the surface. Under this condition, if an oil droplet is placed on the surface, the oil droplet would reside in the Cassie state (Li et al. 2018a; Zhou

et al. 2018). The relationship between superhydrophilicity and underwater superoleophobicity can be explained by the following Young–Dupré equation (Zhou et al. 2018).

$$Cos\,\theta_{OW} = \frac{\gamma_{OA}Cos\,\theta_{OA} - \gamma_{WA}Cos\,\theta_{WA}}{\gamma_{OW}} \quad (1)$$

where γ_{OW}, γ_{OA} and γ_{WA} are the interfacial tension of an oil–water interface, surface tension of oil and surface tension of water, respectively. θ_{OA}, θ_{WA} and θ_{OW} are the contact angles of oil in air, water in air and oil in water, respectively. As predicted by Eq. (1), the value of $\gamma_{OA}Cos\,\theta_{OA} - \gamma_{WA}Cos\,\theta_{WA}$ is commonly negative, since the surface tension of water is much higher than that of the oil/organic solvents. Thus, the hydrophilic surface in the air will show oleophobicity in water.

In this work, underwater oil contact angle (OCA) on WPPP layer surface was also examined. When an underwater oil droplet is placed onto the surface of WPPP layer, the oil droplet acquires approximately spherical in shape, which implies underwater oleophobicity of the WPPP, as shown in Fig. 4c (diesel oil

droplet). Furthermore, the underwater OCA on the surface of WPPP layer was evaluated for a series of oils (hexane, toluene, dodecylbenzene, diesel, and kerosene). As displayed in Fig. 4d, the OCA values for these oils ranged from 147.2° to 152.4°. This observation indicates that in underwater condition, oil wettability of WPPP layer surface changes from oleophilicity to superoleophobicity. This observed underwater superoleophobicity may be attributed to the intrinsically superhydrophilic nature of potato peels materials in air, which consists of starch and cellulose (Li et al. 2016). Due to these specific components, potato peels have excellent water trapping, absorbing and retaining capacities. Because of its nature, a water film is formed on the surface of the WPPP layer under water which reduces the contact between oily liquids and WPPP layer. The three-phase system, oil/water/WPPP layer, behaves like an oil (non-polar) repellent material and prevents oil droplets from coming into contact with the surface of WPPP layer. The Gibbs free energy (ΔG) required to replace the solid-water interface by a solid-oil interface can be expressed as (Fu et al. 2018):

$$\Delta G = \frac{(\gamma_{SW} - \gamma_{SO})(\cos \theta_0 - 1)}{\cos \theta_0} \qquad (2)$$

According to the Eq. (2), for a favourable and thermodynamically feasible process of replacement of water on a solid surface by the oil, ΔG should be < 0 and the contact angle of oil, θ_0, should be $< 90°$. However, according to our experimental observation, the values of underwater oil contact angle were ranged from 147.2° to 152.4°. The results of the study imply that the water film on the surface of the WPPP layer cannot be replaced easily by the oily liquids. Thus, it can be concluding that the underwater oleophobicity of the solid surfaces increases with its hydrophilicity in the air (Zhou et al. 2018).

We also studied the water affinity of NaClO$_2$ treated and untreated WPPP by the measurement of water absorbing ability. The water absorption ratio of NaClO$_2$ treated and untreated WPPP was about 194.8 wt% and 172.4 wt%, respectively. This indicates that NaClO$_2$ treated WPPP has better water affinity than the untreated WPPP. Therefore, owing to its underwater superoleophobicity the NaClO$_2$-treated WPPP can be used as a superior candidate for filtrate membrane to selectively remove oil from various oil/water mixtures through the filtration process.

Potential application in immiscible oil/water separation

The separation and clean-up of oily pollutants from water have become major environmental issues all around the world because of regular oil-contamination (Singh and Singh 2017b). The as-constructed NaClO$_2$-treated WPPP layer surface was used as a selective filter to separate oils or organic solvents from a series of oil/water mixtures. If the NaClO$_2$-treated WPPP layer is prewetted with water, it allows only water to pass through the layer, while oil is repelled. By taking the advantage of this, we evaluated the separation capacity of NaClO$_2$-treated WPPP for a series of oil/water mixtures (1:1 volume ratio) including hexane, toluene, dodecylbenzene, kerosene, diesel/water mixtures via simple filtration approach, as shown in Fig. 5. It was observed that upon pouring a diesel-water mixture onto the WPPP layer, which was prewetted with water, water immediately passed through the WPPP layer owing to its excellent water affinity, whereas the diesel oil (light yellowish color) was blocked and retained on the upper surface of wetted WPPP layer in the column (Video S1). Interestingly, the separated oily liquid can stand on WPPP layer for 2 h without any permeation. Moreover, in the filtered water, no visible diesel oil was observed, thus further ensuring its excellent oil–water separation capability (Fig. 5 a, b).
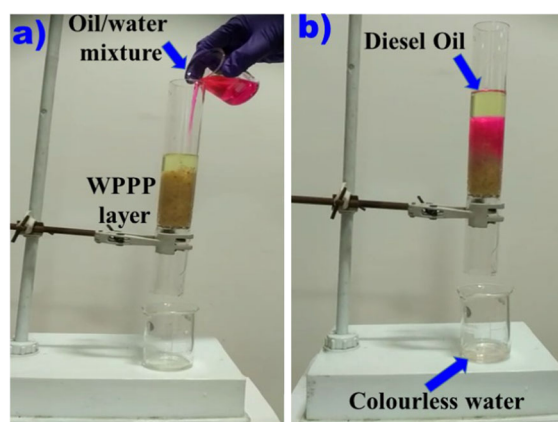

Fig. 5 a, **b** Illustration of the procedures of immiscible oil/water mixtures (v/v, 1:1) separation through pre-wetted WPPP layer (as a filtrate material). Water was dyed with rhodamine B

We further examined the possibility of the oil content in the filtrate with another oil/water mixture in which oil was pre-dyed with Sudan blue II. After several cycles of oil/water separation process, it was observed that no part of the WPPP layer being stained with oil-soluble dyes as oil was repelled by the trapped water cushion in the microstructures of the WPPP. A similar observation has been reported earlier for the separation of oil/water mixtures using an underwater superoleophobic wood sheet, walnut shell layer and coconut shell layer (Yong et al. 2018; Li et al. 2017a, 2018b).

In addition, separation of some other oil–water mixtures (hexane, toluene, dodecylbenzene, and kerosene) has also been evaluated with the as-constructed WPP layer by the similar separation phenomenon. We observed that these oils are also successfully separated similar to the diesel oil–water mixture through the ordinary gravity-directed filtration approach.

The efficiency of the as-prepared WPPP for all oils were determined by the calculation of the oil rejection coefficient (R%) according to the following equation (Cao et al. 2016):

$$R(\%) = \left(1 - \frac{C_p}{C_0}\right) \times 100$$
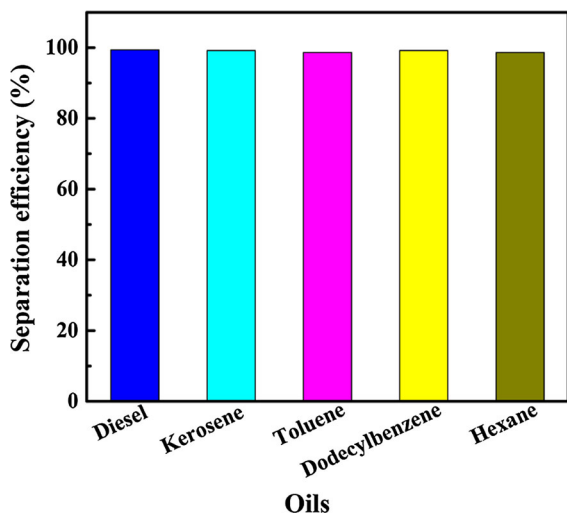
where C_P is the weight of oil collected after oil–water separation, and C_0 is the weight of oil before oil–water separation. As shown in Fig. 6, the treated WPPP layer exhibited high oil–water separation efficiency (> 98%) for all selected oils, even after 10 repeated cycles of filtration process at ambient temperature. This observation inferred its efficient recyclability for the oil–water separation application.

Sometimes oil-contaminated water may exist in a saline environment. As we have seen, during the oil/water separation process, the as-prepared WPPP layer is fully wetted with water. Thus the stability of such materials is essential along with its superhydrophilicity and underwater superoleophilicity under saline conditions. To this end, we also studied the stability of the as-prepared WPPP in a saline environment by evaluating its separation efficiency for diesel oil–water (20 mL of 1:1 v/v) mixtures in the presence of high salt concentration (1.0%, 2.0% and 3.5% of NaCl) in water, which was repeated up to 10 cycles. It was observed that separation efficiency was greater than 98% which is as high as observed for other simple oil–water mixtures without salt concentration. This demonstrates the stability of material property under such saline conditions.

### Application in gravity-directed water-in-oil emulsions separation

The separation of emulsified oil–water mixtures is more difficult as compared to the separation of regular immiscible oil–water mixtures. This is primarily due to the variable nature of the disperse phase. In the case of immiscible oil–water mixtures, the diameter of the disperse phase is generally > 150 μm (Li et al. 2017a, b), consequently, the separation of simple oil–water mixtures is relatively easier. However, the difficulty is significantly higher in case of oil/water emulsion where the disperse phase particle size generally < 20 μm (Lin et al. 2016). The as-prepared WPPP layer possesses simultaneously the property of superhydrophilicity and underwater superoleophobicity, which was achieved by prewetting of the WPPP layer with water. By virtue of its specific property, the WPPP layer prewetted with water can effectively separate oil/water mixtures because the oil gets repelled by the trapped water cushion in the microstructure of the WPPP, preventing the direct

Fig. 6 Separation efficiency of various oil/water mixtures (V/V, 1:1, 200 mL) through pre-wetted WPPP layer (as a filtrate material)

contact between oil and WPPP surface (Cheng et al. 2017).

However, the separation of oil/water mixture is not possible by WPPP layer prewetted with oil. Under such condition (prewetted with oil), the WPPP layer exhibited underoil superhydrophilicity, which suggests that in oil-rich environments, the WPPP layer has ability to adsorbs water droplets. It is well known that for the separation of oil/water emulsion filtering material should have high resistance for the dispersed phase and high wettability for continuous phase (Wang and Wang 2018). Thus, it can be useful in separating water-in-oil emulsion in oil-rich environments. (Li et al. 2018c). To assess the emulsified oil/water separation ability of the as-prepared WPPP layer, water-in-oil emulsions including water-in-toluene and water-in-dodecylbenzene were prepared. The as-similar procedure for the separation of immiscible oil/water mixture, emulsified solution was poured onto the WPPP layer. It was observed that

water-in-toluene and water-in-dodecylbenzene emulsions were separated successfully (driven only by gravity) with good flux and single step procedure (Video S2). The droplets of water in emulsions before and after filtration were analyzed using optical microscopy characterization. As shown in Fig. 7a, b, the optical microscopy images and digital photographs ($7a_{ii, iii}$, $b_{ii, iii}$) reveal the phase composition difference between the prepared emulsions and their respective collected filtrate.

Figure 7a, b, shows that the as-prepared emulsions were in milky appearance due to tiny size water droplets as the disperse phase. On the other hand, the prepared emulsion passes through the WPPP layer, the collected filtrate appears as transparent and no water droplets were observed in optical microscopic images of filtrate. Water droplets rapidly adsorb through the WPPP layer and thus original milky emulsion converts into a transparent filtrate. This observation indicates efficient removal of water from surfactant-free water-
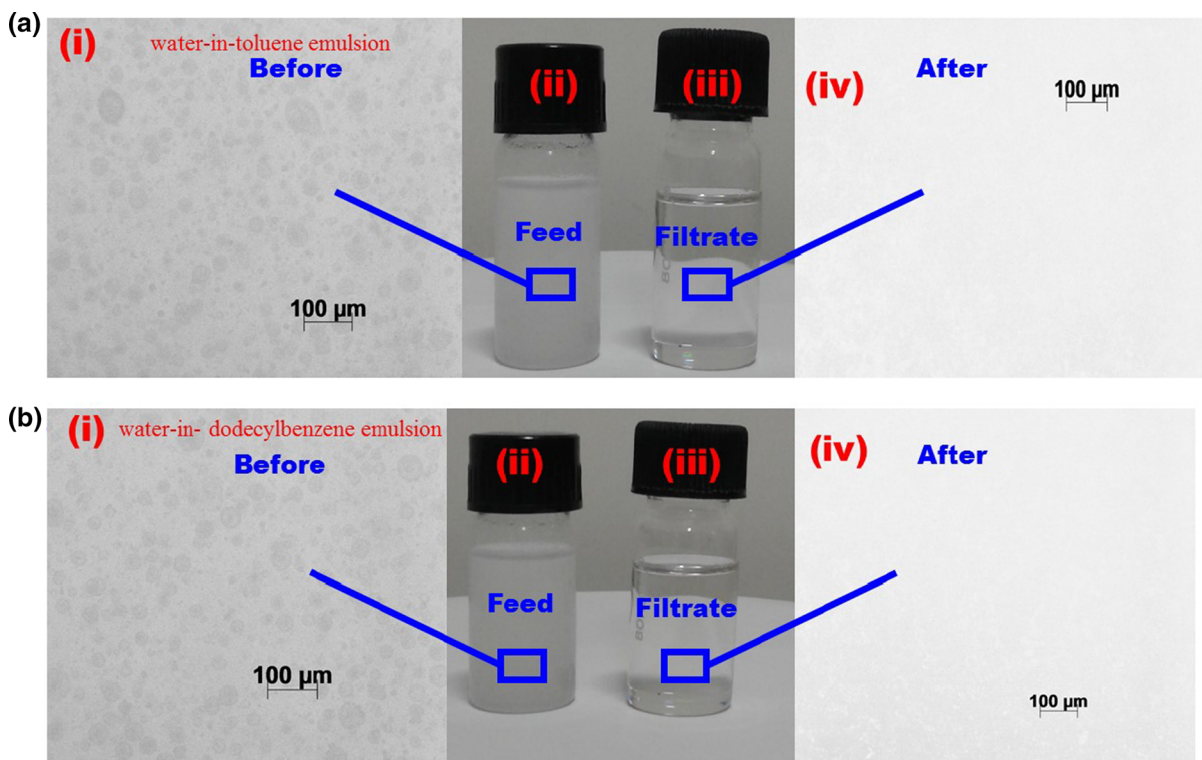
Fig. 7 a Optical microscopic images (i, iv) and digital photos (ii, iii) of the water-in-toluene emulsion before and after filtering through the as-prepared WPPP layer. **b** Optical microscopic images (i, iv) and digital photos (ii, iii) of the water-in-dodecylbenzene emulsion before and after filtering through the as-prepared WPPP layer

in-oil emulsions through the ordinary gravity-driven filtration process using the WPPP layer. This is mainly due to the porous structure and complex hydrophilic components of WPP particles providing the WPPP layer an excellent under oil superhydrophilicity, which could effectively adsorb water droplets from the emulsion. Similar behavior of the removal of water from the water-in-oil emulsions by the use of under oil superhydrophilic materials has been reported earlier owing to its complex hydrophilic components (Li et al. 2018b, c).

In order to ascertain the fluxes for water-in-oil emulsions through the WPPP layer Eq. (3) is used:

$$\text{Flux} = \frac{V}{At} \qquad (3)$$

where V is the volume (0.1 L) of oil–water emulsion, A is the effective filtration area of the WPPP surface and t is the required time for the permeation of water-in-oil emulsions. During the flux calculation, 0.1 L of the emulsion was poured on the WPP surface and permeation time was noted. This process was repeated three times to get an average value. The flux was larger than 2 L $m^{-2}s^{-1}$ for both emulsions.

Application of WPPP for water-soluble dyes removal during oil/water separation

As is well known, water-soluble dyes are also one of the most serious water pollutants because of its persistence and toxicity (Yimina et al. 2018; Guo et al. 2017). The presence of water-soluble dyes with an insoluble oil in water affects the human health enormously (Zhu et al. 2017). To this end, the separation performance of the NaClO$_2$-treated WPPP for water-soluble dyes with oil/water mixtures was also examined. In the dye adsorption experiment, rhodamine B and methylene blue dyes were used as target contaminants to evaluate the adsorption of water-soluble dyes during oil/water separation simultaneously. In this process, initially, the mixture (50%, v/v) of diesel oil and water (dyes with methylene blue, 50 mg L^{-1}) was prepared and passed through the surface of prewetted WPPP layer as shown in Fig. 8. It was observed that after one-time permeate, the methylene blue dyed water become colorless and no oil was visible to naked eyes in the collected filtrate,

demonstrating the excellent adsorption capacity of the WPPP layer for the water-soluble dyes (Fig. 8a–c).

Furthermore, to confirm these results, UV–Vis spectrophotometer was used to analyze the change in MB concentration by the recording of UV–Vis spectra of the solution before and after the filtration process. It can be seen from Fig. 9a, that before filtration, MB contaminated water showed a strong peak at 664 nm aqueous solution. However, after one-time permeation through the WPPP layer, the corresponding peak of the MB dyed contaminated water (50 mg L^{-1}) was completely disappeared, demonstrating the excellent adsorption efficiency for MB in water. In addition, repeatability of dye adsorption from MB contaminated water by the WPPP layer was also evaluated. In this experiment, 20 mL of oil/water mixtures (1:1, v/v) was used with 50 mg L^{-1} of dye concentration in water. After the 10 successive gravity driven filtration process it was observed that water-soluble MB dyes were completely adsorbed in each cycle by the WPPP layer without any appearance of dye color in the filtrate. Thus, all these results of the study imply that WPPP layer exhibits rapid and excellent adsorption performance for MB dye during the oil/water separation simultaneously. We assumed that the reason behind this phenomenon is the high concentration of hydroxyl group on the surface of NaClO$_2$-treated WPPP. As observed in FT-IR spectra (Fig. 3) of the as-treated WPPP, the peak intensity at 3408 cm^{-1} indicating the exposure of hydroxyl groups. Thus N atoms of dyes in water can form the hydrogen bond with the hydroxyl groups on the modified WPPP surface, which can capture dye contaminants and responsible for the high adsorption capacity of WPPP (Qu et al. 2018). In addition to this, the porous surface structure of the WPPP is useful to capture the water-soluble dyes by the physical adsorption process (Guechi and Hamdaoui 2016).

Meaningful dye adsorbents are those which can be applied not only to a specific dye but also should have the ability to adsorb other kinds of dyes. Thus, in order to evaluate the separation performance of the modified WPPP with respect to other dyes, we consider two cases viz., a) 50 mg L^{-1} rhodamine B (Rh-B) and b) a mix solution of MB with Rh-B (50 mg L^{-1} of each dye). Subsequently, the water-soluble dye absorption capability of the WPPP in these solutions was examined via gravity-driven filtration approach.
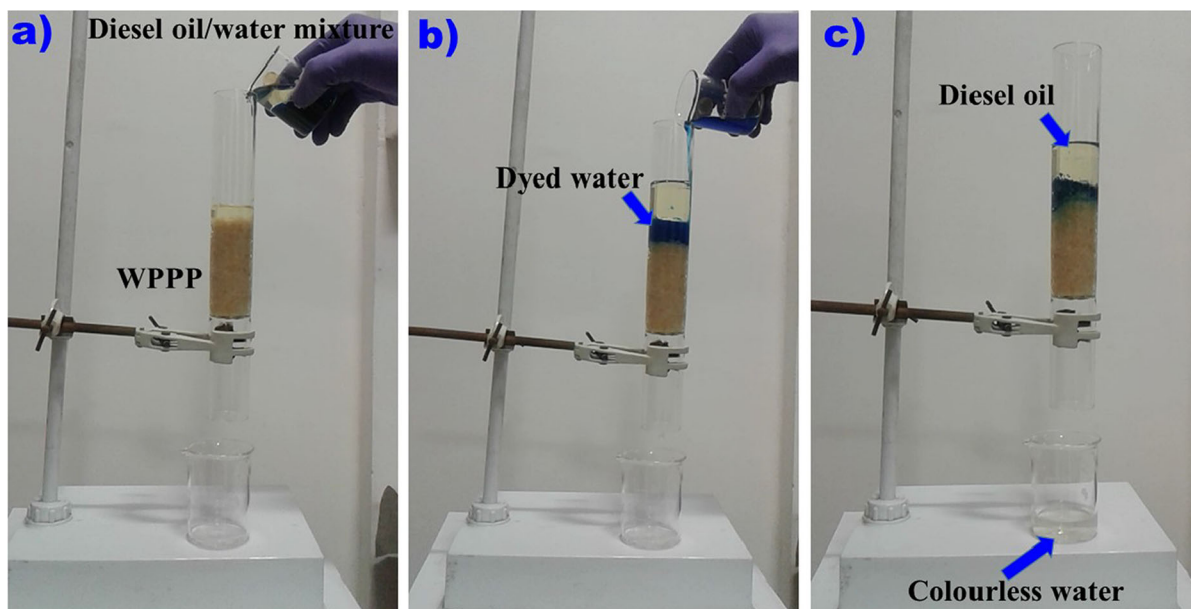
Fig. 8 **a**, **b** and **c** Separation and adsorption processes of water-soluble methylene blue dye (50 mg L^{-1}) during oil/water separation process using pre-wetted WPPP layer

Figure 9b, c showed the UV–Vis spectra of Rh-B, and the mixture solution of Rh-B with MB before and after the one-time filtration process. Initially, before filtration, the Rh-B solution showed a strong peak (maximum absorption) at 554 nm, while a strong peak for MB was observed at 664 nm. Based on the UV–Vis spectra, it is clear that the treated WPPP has an excellent adsorption capability for Rh-B dye individually as well as also in the presence of MB dye of equal concentration (50 mg L^{-1} each) during the process of oil/water separation.
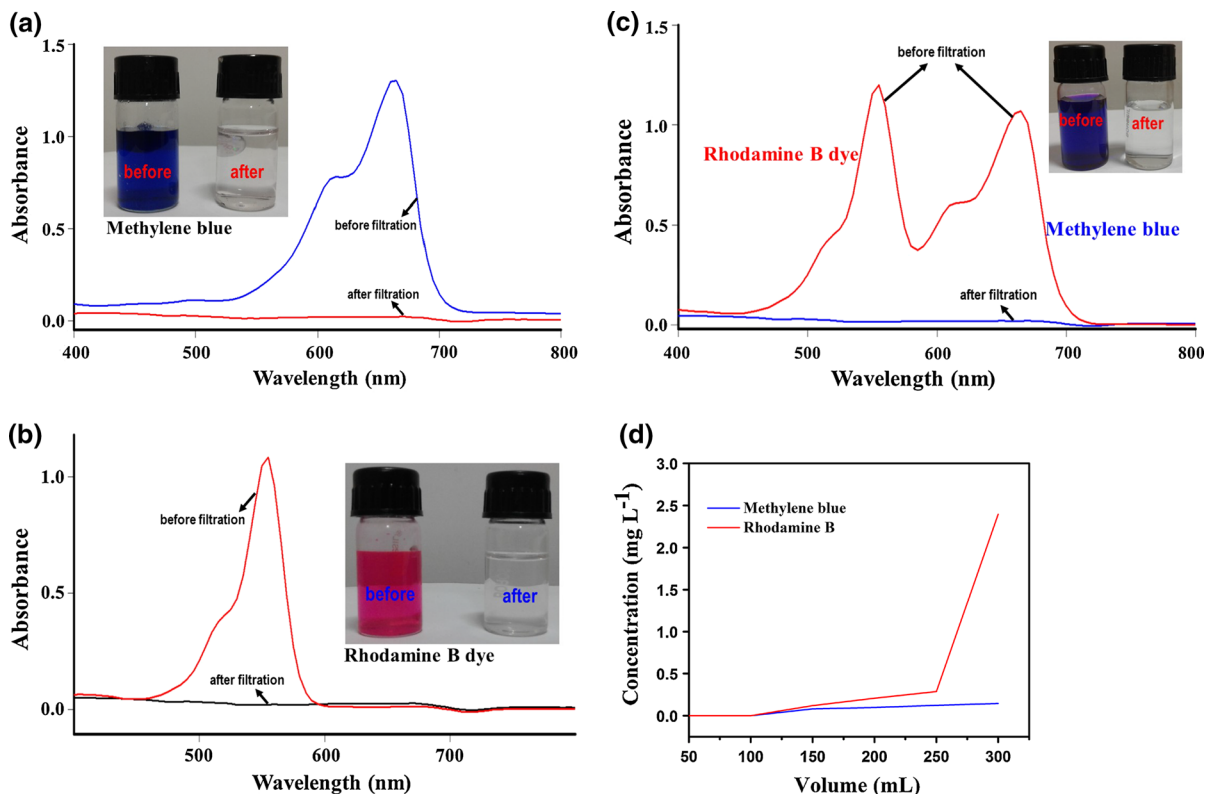
The inset photographs of Fig. 9b, c show that the original dye solution of Rh-B and mix solution of Rh-B and MB became colourless and transparent after one step filtration process.

In order to further evaluate the maximum dye adsorption capacity (q_{max}) of the WPPP, the same concentration (50 mg L^{-1}) of Rh-B and MB solution were used. The adsorption capacity for each type of dye was calculated according to the following equation (Li et al. 2017a):

$$q_{max} = \frac{C_i V_f}{M} - \frac{1}{M} \int_0^{V_f} C(V) \, dV \qquad (4)$$

where, M is the mass (g) of WPPP layer, C_i (mg L^{-1}) is the initial concentration of dye, V_f is the total volume of the dye solution through the WPPP layer,

and C(V) is the concentration of dye in the filtrate for a given volume of the dye solution. In the test, 300 mL of oil/water mixtures (1:1, v/v) (C_i, 50 mg L^{-1} of dye concentration) was passed through the surface of prewetted WPPP layer (5 g, mass) as shown in Fig. 8. The final concentration of dye, C(V), was measured in the collected filtered water after one time permeate at every 50 mL volume. Therefore, as shown in Fig. 9d, the final concentration of both dyes in every cycle was lower than 2.5 mg L^{-1}. This result demonstrates that the WPPP layer exhibited rapid and excellent adsorption efficiency after one time permeate for the MB and Rh-B dye by reducing the dye concentration from 50 mg L^{-1} to 0.2 mg L^{-1} (99.6%) and 2.4 mg L^{-1} (95.2%), respectively. However, the dye adsorption capacity of the WPPP in terms of mg g^{-1} is dependent on the thickness and mass of the WPPP layer. Thus for 5 grams of the WPPP layer, the MB and Rh-B dye adsorption capacities were 2.99 and 2.98 mg g^{-1}, respectively. From the above observation of results, it is evident that the as-prepared WPPP has excellent efficiency for the simultaneous removal of water-soluble dyes and insoluble oils from water, exhibiting its promising ability for treatment of water pollution.

Fig. 9 **a** UV–vis absorption spectra of methylene blue (blue line) and after one-time adsorption filtrate (red line). The inset photographs illustrate that the original methylene blue solution became clear and colorless after adsorption via one-time filtration process. **b** UV–vis absorption spectra of Rhodamine B dye (red line) and after one-time adsorption filtrate (black line). The inset photographs illustrate that the rhodamine B dye solution became clear and colorless after adsorption via one-time filtration process. **c** UV–vis absorption spectra of the initial mixture of rhodamine B with methylene blue (50 ppm each) was colored (red line in spectra) and became clear and colourless (blue line) after adsorption via one-time filtration process. **d** The relationship between the final concentration of water soluble pollutants (methylene blue and rhodamine B dyes) and pollutants liquid volume. (Color figure online)

Conclusions

In this work, we have demonstrated the development of a green and extremely low cost WPPP layer with superhydrophilicity and underwater superoleophobicity from waste potato peels by one step $NaClO_2$ treatment. By virtue of its specific wettability, the as-prepared WPPP materials layer exhibit excellent capability to separate a series of oil/water mixtures including water-in-oil emulsions in just a single step permeation process with high efficiency ($> 98.6\%$). Furthermore, the WPPP layer was also effective for the adsorptive separation of water-soluble dyes of high concentration (50 mg L^{-1}) during oil/water separation, simultaneously via a simple gravity directed separation approach. Thus, these excellent performances emphasize the practical importance of the waste-derived materials for diversified application in water remediation. We believe that the development of superhydrophilic and underwater superoleophobic WPPP layer from waste potato peels will not only contribute in reducing environmental pollution but also have attractive features as a promising material for water purification.

References

Arampatzidou AC, Deliyanni EA (2016) Comparison of activation media and pyrolysis temperature for activated carbons development by pyrolysis of potato peels for effective adsorption of endocrine disruptor bisphenol-A. J Colloid Interface Sci 466:101–112

Baig U, Matin A, Gondal MA, Zubair SM (2018) Facile fabrication of superhydrophobic, superoleophilic photocatalytic membrane for efficient oil-water separation and removal of hazardous organic pollutants. J Clean Prod. https://doi.org/10.1016/j.jclepro.2018.10.079

Camire ME, Violette D, Dougherty MP, McLaughlin MA (1997) Potato peel dietary fiber composition: effects of peeling and extrusion cooking processes. J Agric Food Chem 45:1404–1408

Cao Y, Liu N, Zhang W, Feng L, Wei Y (2016) One-step coating toward multifunctional applications: oil/water mixtures and emulsions separation and contaminants adsorption. ACS Appl Mater Interfaces 8:3333–3339

Cheng Q, Ye DD, Chang C, Zhang L (2017) Facile fabrication of superhydrophilic membranes consisted of fibrous tunicate cellulose nanocrystals for highly efficient oil/water separation. J Membr Sci 525:1–8

Das S, Kumar S, Samal SK, Mohanty S, Nayak SK (2018) A review on superhydrophobic polymer nanocoatings: recent development and applications. Ind Eng Chem Res 57:2727–2745

Feng Y, Wang Y, Wang Y, Yao J (2017) Furfuryl alcohol modified melamine sponge for highly efficient oil spill clean-up and recovery. J Mater Chem A 5:21893–21897

Fu S, Zhou H, Wang H, Niu H, Yang W, Shaoa H, Lin T (2018) Amphibious superamphiphilic fabrics with self-healing underwater superoleophilicity. Mater Horiz. https://doi.org/10.1039/c8mh00898a

Gao X, Jiang L (2004) Water-repellent legs of water striders. Nature 432:36

Guechi E-K, Hamdaoui O (2016) Biosorption of methylene blue from aqueous solution by potato (*Solanum tuberosum*) peel: equilibrium modelling, kinetic, and thermodynamic studies. Desalin Water Treat 57:10270–10285

Guo F, Wen Q, Guo Z (2017) Low cost and non-fluoride flowerlike superhydrophobic particles fabricated for both emulsions separation and dyes adsorption. J Colloid Interface Sci 507:421–428

Khosravi M, Azizian S (2017) Preparation of superhydrophobic and superoleophilic nanostructured layer on steel mesh for oil–water separation. Sep Purif Technol 172:366–373

Li J, Li D, Yang Y, Li J, Zha F, Lei Z (2016) A prewetting induced underwater superoleophobic or underoil (super) hydrophobic waste potato residue-coated mesh for selective efficient oil/water separation. Green Chem 18:541–549

Li J, Zhao Z, Li D, Tang X, Feng H, Qi W, Wang Q (2017a) Multifunctional walnut shell layer used for oil/water mixtures separation and dyes adsorption. Appl Surf Sci 419:869–874

Li Y, Zhang Z, Ge B, Men X, Xue Q (2017b) A versatile and efficient approach to separate both surfactant-stabilized water-in-oil and oil-in-water emulsions. Sep Purif Technol 176:1–7

Li C, Lai H, Cheng Z, Yan J, An M (2018a) Designing robust underwater superoleophobic microstructures on copper substrates. Nanoscale 10:20435–20442

Li J, Xu C, Zhang Y, Tang X, Qi W, Wang Q (2018b) Gravity-directed separation of both immiscible and emulsified oil/water mixtures utilizing coconut shell layer. J Colloid Interface Sci 511:233–242

Li J, Xu C, Guo C, Tian H, Zha F, Guo L (2018c) Underoil superhydrophilic desert sand layer for efficient gravity-directed water-in-oil emulsions separation with high flux. J Mater Chem A 6:223–230

Lin X, Heo J, Jeong H, Choi M, Chang M, Hong J (2016) Robust superhydrophobic carbon nanofiber network inlay-gated mesh for water-in-oil emulsion separation with high flux. J Mater Chem A 4:17970–17980

Linag S, McDonald AG (2014) Chemical and thermal characterization of potato peel waste and its fermentation residue as potential resources for biofuel and bioproducts production. J Agric Food Chem 62:8421–8429

Liu BM, Wang S, Wei Z, Song Y, Jiang L (2009) Bioinspired design of a superoleophobic and low adhesive water/solid interface. Adv Mater 21:665–669

Liu X, Zhou J, Xue Z, Gao J, Meng J, Wang S, Jiang L (2012) Clam's shell inspired high-energy inorganic coatings with underwater low adhesive superoleophobicity. Adv Mater 24:3401–3405

Marmur A (2012) Hydro-hygro-oleo-omni-phobic? Terminology of wettability classification. Soft Matter 8:6867–6870

Nguyen T-B, Park S, Lim H (2018) Effects of morphology parameters on anti-icing performance in superhydrophobic surfaces. Appl Surf Sci 435:585–591

Qu M, Ma L, Zhou Y, Zhao Y, Wang J, Zhang Y, Zhu X, Liu X, He J (2018) Durable and recyclable superhydrophilic-superoleophobic materials for efficient oil/water separation and water-soluble dyes removal. ACS Appl Nano Mater 1:5197–5209

Schlaich C, Camacho LC, Yu L, Achazi K, Wei Q, Haag R (2016) Surface-independent hierarchical coatings with superamphiphobic properties. ACS Appl Mater Interfaces 8:29117–29127

Si Y, Dong Z, Jiang L (2018) Bioinspired designs of superhydrophobic and superhydrophilic materials. ACS Cent Sci 4:1102–1112

Singh JK, Muller-Plathe F (2014) On the characterization of crystallization and ice adhesion on smooth and rough surfaces using molecular dynamics. Appl Phys Lett 104:021603

Singh AK, Singh JK (2016) Fabrication of zirconia based durable superhydrophobic–superoleophilic fabrics using non fluorinated materials for oil–water separation and water purification. RSC Adv 6:103632–103640

Singh AK, Singh JK (2017a) Fabrication of durable superhydrophobic coatings on cotton fabrics with photocatalytic activity by fluorine-free chemical modification for dual-functional water purification. New J Chem 41:4618–4628

Singh AK, Singh JK (2017b) Fabrication of durable super-repellent surfaces on cotton fabric with liquids of varying surface tension: low surface energy and high roughness. Appl Surf Sci 416:639–648

Singh AK, Singh JK (2019) An efficient use of waste PE for hydrophobic surface coatings and its application on cotton fibers for oil–water separator. Prog Org Coat 131:301–310

Singh AK, Ketan K, Singh JK (2017) Simple and green fabrication of recyclable magnetic highly hydrophobic sorbents derived from waste orange peels for removal of oil and organic solvents from water surface. J Environ Chem Eng 5:5250–5259

Song J, Wang D, Hu L, Huang X, Chen Y (2018) Superhydrophobic surface fabricated by nanosecond laser and perhydropolysilazane. Appl Surf Sci 455:771–779

Sukamanchi R, Mathew D, Kumar KSS (2017) Durable superhydrophobic particles mimicking leafhopper surface: superoleophilicity and very low surface energy. ACS Sustain Chem Eng 5:252–260

Ueda E, Levkin PA (2013) Emerging applications of superhydrophilic-superhydrophobic micropatterns. Adv Mater 25:1234–1247

Wang J, Wang H (2018) Easily enlarged and coating-free underwater superoleophobic fabric for oil/water and emulsion separation via a facile NaClO$_2$ treatment. Sep Purif Technol 195:358–366

Wen X, Liu H, Zhang L, Zhang J, Fu C, Shi X, Chen X, Mijowska E, Ming-Jun Chen M-J, Wang D-Y (2019) Large-scale converting waste coffee grounds into functional carbon materials as high-efficient adsorbent for organic dyes. Bioresour Technol 272:92–98

Yimina D, Jiaqi Z, Danyang L, Lanli N, Liling Z, Yi Z, Xiaohong Z (2018) Preparation of Congo red functionalized Fe$_3$O$_4$@SiO$_2$ nanoparticle and its application for the removal of methylene blue. Colloids Surf A 550:90–98

Yong J, Chen F, Huo J, Fang Y, Yang Q, Bian H, Li W, Wei Y, Dai Y, Hou X (2018) Green, biodegradable, underwater superoleophobic wood sheet for efficient oil/water separation. ACS Omega 3:1395–1402

You Q, Ran G, Wang C, Zhao Y, Song Q (2018) A novel superhydrophilic–underwater superoleophobic Zn–ZnO electrodeposited copper mesh for efficient oil/water separation. Sep Purif Technol 193:21–28

Zhan H, Zuo T, Tao R, Chang C (2018a) Robust tunicate cellulose nanocrystal/palygorskite nanorod membranes for multifunctional oil/water emulsion separation. ACS Sustain Chem Eng 6:10833–10840

Zhan H, Peng N, Lei X, Huang Y, Li D, Tao R, Chang C (2018b) UV-induced self-cleanable TiO2/nanocellulose membrane for selective separation of oil/water emulsion. Carbohydr Polym 201(2018):464–470

Zhang Z, Luo X, Liu Y, Zhou P, Ma G, Lei Z, Lei L (2015) A low cost and highly efficient adsorbent (activated carbon) prepared from waste potato residue. J Taiwan Inst Chem Eng 49:206–211

Zhou H, Zhao Y, Wang H, Lin T (2016) Recent development in durable super-liquid-repellent fabrics. Adv Mater Interfaces 3:1600402

Zhou C, Feng J, Cheng J, Zhang H, Lin J, Zeng X, Pi P (2018) Opposite superwetting nickel meshes for on-demand and continuous oil/water separation. Ind Eng Chem Res 57:1059–1070

Zhu H, Chen D, Li N, Xu Q, Li H, He J, Lu J (2017) Dual-layer copper mesh for integrated oil–water separation and water purification. Appl Catal B Environ 200:594–600

Zhu H, Guo P, Shang Z, Yu X, Zhang Y (2018) Fabrication of underwater superoleophobic metallic fiber felts for oil–water separation. Appl Surf Sci 447:72–77